Phase transitions of quasi-two-dimensional antiferroelectric squaric acid ($H_2C_4O_4$) and ($D_2C_4O_4$) investigated by the Green's-function technique

B. K. Chaudhuri and P. K. Dey
Indian Association for the Cultivation of Science, Calcutta 700 032, India

T. Matsuo
Chemical Thermodynamics Laboratory, Faculty of Science, Osaka University, Osaka 560, Japan
(Received 14 July 1989)

The temperature dependences of the dielectric properties at different fixed pressures, and the antiferroelectric phase transitions of squaric acid $H_2C_4O_4$ and its deuterated form $D_2C_4O_4$ have been investigated. Using the four-sublattice pseudospin cluster Hamiltonian, together with a pseudospin-phonon interaction term, the statistical Green's-function technique has been applied to explain phenomenologically the isotope effect, dome-shaped temperature-dependent dielectric constant near the transition temperature T_c and the "crossover" behavior (first order to second order) in $H_2C_4O_4$ crystals. The elongation of the O—H $\cdots$ O bonds alone, contrary to the implication of Samara and Semmingsen [J. Chem. Phys. **71**, 1401 (1979)], is not sufficient to explain the isotope effect and other peculiar features of phase transitions in squaric acid. The model parameters, obtained by fitting the experimental electrical susceptibility data, have also been used to calculate heat capacity ($\bar{C}=A\partial/\partial T[T\chi(T)]$) and reproduces a maximum value of $\bar{C}$ at ≈ 7.0 K above T_c for the $H_2C_4O_4$, which agrees with the corresponding experimental value. From our theoretical observation a unified character of the antiferroelectric transition in $H_2C_4O_4$ and the antiferromagnetic transitions in some two-dimensional Ising systems is well exposed.

I. INTRODUCTION

Squaric acid ($H_2C_4O_4$, hereafter referred to as HSQ) is a moderately strong organic compound first synthesized by Cohen *et al.*[1] Since the discovery of a structural phase transition in this quasi-two-dimensional crystal by Semmingsen and Feder,[2] many experimental techniques have been used to study the nature of this phase transition. Several review articles on the structural and physical properties of HSQ have already been published.[3–5]

Both HSQ and its deuterated form (denoted by DSQ) undergo structural phase transitions (SPT) from monoclinic space group $P2_{1/m}(C_{2h}^2)$ to tetragonal[2–5] space group $I4/m$, respectively, at $T_{cH}=374$ K (for HSQ) and $T_{cD}=516$ K (for DSQ). Although the large isotope effect on the transition temperature T_c (where by T_c we mean both T_{cH} and T_{cD}) suggests an importance of tunneling in HSQ via its similarity with the KH_2PO_4 (KDP) type H-bonded crystals,[6] recent dielectric studies under pressure by Samara and Semmingsen[7] did not, however, attribute much importance to the tunneling effect. In particular, using the pure-pseudospin model, viz.,

$$H=-\Omega\sum_i X_i-\tfrac{1}{2}\sum_{ij}J_{ij}Z_iZ_j \qquad (1)$$

(where Ω is the tunneling frequency, J is the exchange integral, and X_i, Z_i, etc. are the x, z, etc. components of the pseudospin variable S), the large isotope effect on T_c was considered by them[7] to be due to the large difference in the hydrogen-bond distances between the HSQ and DSQ samples. The hydrogen-bond (O—H $\cdots$ O) length (Fig. 1) in HSQ is $R_{O\_O}=2.554$ Å, which is quite large for a hydrogen bond, and the distance between the two states of proton equilibrium[8] $R_H\approx 0.486$ Å (is fully 38% larger in KDP).

Yasuda *et al.*,[9] however, found that the value of $d\ln T_{cH}/dp$ (where p is the pressure) for HSQ is about -3.5%/kbar and is comparable with the values of $d\ln T_{cH}/dp=-3.78\%$/kbar and -4.4%/kbar, respectively, for the H-bonded $NH_4H_2PO_4$ (ADP) and

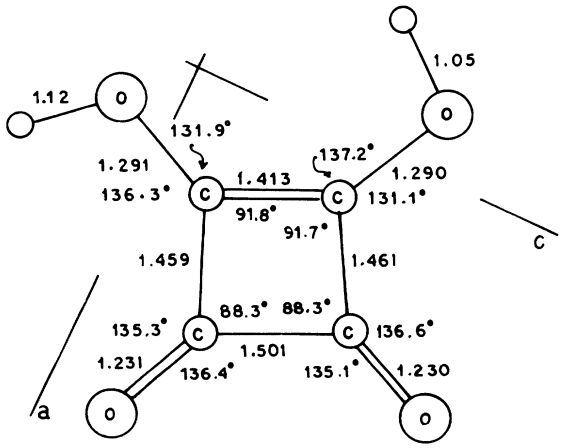

FIG. 1. Bond length (in Å) and angles in squaric acid (HSQ) (Refs. 6 and 9).

 ©1990 The American Physical Society

RbH_2PO_4 (RDP). In all the above crystals the tunneling term was considered to be an important parameter. Again the ratio T_{cD}/T_{cH} (=1.38) for HSQ is also comparable with those of KDP (T_{cD}/T_{cH}=1.81) and ADP (T_{cD}/T_{cH} =1.59) crystals. Similar to the KDP crystal a marked expansion of about 0.03 Å of the O—H $\cdots$ O bond length on deuteration was also observed for the HSQ crystal. Thus HSQ- and the KDP-type H-bonded crystals behave almost similarly.

In their theoretical models Eatsushita *et al.*[10] and Zinenko[11] emphasized the tunneling term to study the dielectric properties of HSQ and DSQ. On the other hand, Schneider and Tornau[12] investigated the transition in HSQ by considering a five-particle cluster approximation without paying much attention to the tunneling motion of protons. However, all of these proposed pseudospin models, together with that given by Eq. (1) (or its modifications[10–12]), which have been applied for the explanation of the higher phase transition temperature in the deuterated HSQ crystal, we believe to be incomplete. This is because of the fact that the pseudospin-phonon contribution, neglected in the above models, has been reported[13–16] to be very important for understanding most of the salient features of structural phase transitions in H-bonded crystals.

It was also pointed out earlier by several authors[2–5,17] that HSQ is a two- or quasi-two-dimensional hydrogen-bonded (H-bonded) compound generally believed to undergo a continuous phase transition. The ^{13}C NMR spectra obtained by Mehring and Suwelack[18,19] showed cluster phenomena and a discontinuous jump in the order parameter at T_{cH}. They assumed[18,19] that the phase transition in HSQ might be of first order in nature. Kuhn *et al.*[20] subsequently concluded from their birefringence data that the transition could be described by the Landau theory of first-order phase transitions. Thus evidence for both first- and second-order nature of SPT in HSQ is found from the current literature survey. Meanwhile an interesting "crossover" from first- to second-order transition induced by a symmetry-breaking field for the $n=2$ model has been proposed recently by Kerszberg and Mukamel[21] (where n is the effective number of components of the order parameter). Observation of the crossover phenomenon in HSQ further demands critical theoretical analysis of the transition mechanism in this crystal.

Another interesting unexplained behavior of this HSQ salt is the appearance of the antiferromagnetic (AFM) type dome-shaped dielectric constant $\epsilon_a'(T)$ curve with a maximum at 7.5 K above T_{cH} and 5.0 K above T_{cD} (Ref. 7). Other examples for which a maximum in $\epsilon_a'(T)$ (dielectric constant along the a axis) above T_c has also been observed in the transverse dielectric constant include KDP,[22] the 1D antiferrolectric Jahn-Teller $PrCl_3$,[23] and the 186 K displacive antiferrodistortive transition in $KMnF_3$,[24] etc. To throw more light on the unified character of the above phase transition in these crystals along with HSQ is also one of the motivations of our present theoretical investigation with the pseudospin-lattice coupled-mode Hamiltonian of the form already discussed by us.[13–16] An attempt has also been made to study the anomalous dielectric behavior of HSQ with the hydrostatic pressure dependences of the dielectric constants (ϵ_a') along the a axis.[7,9] The values of ϵ_a' increase monotonically with increasing pressure. The value of $(d\epsilon_a'/dp)$ becomes a maximum at $p=p_{max}$. After that, ϵ_a' displays a broad flat maximum and decreases gradually with pressure. Such a behavior of ϵ_a' with pressure is quite analogous[7,9] to that of ϵ_a' with temperature (see also Fig. 5 of this paper). Thus the phases at $p<p_{max}$ and $p>p_{max}$ might be compared with those phases at $T<T_{max}$ and $T>T_{max}$, respectively. Therefore we may regard p_{max} as a transition pressure. We further assumed that the same type of model could be used for the study of both pressure and temperature dependences of the dielectric properties of HSQ with different sets of model parameters.

The above-mentioned pseudospin model used by us for the study of the phase transition in HSQ is a four-sublattice pseudospin cluster Hamiltonian coupled with phonon-phonon interaction terms. We shall show that with such a model Hamiltonian the crossover behavior, dome-shaped electrical susceptibility (χ_a) above T_c, and very close similarly in the behavior of the electrical susceptibility of HSQ with that of the magnetic susceptibility of some two-dimensional Ising antiferromagnetic materials can be phenomenologically explained from the common standpoint.

For a better understanding of the mechanism of phase transition in HSQ and also for developing the pseudospin-phonon coupled Hamiltonian we discuss below the crystal structure and the hydrogen-bond arrangements of HSQ in some detail.

Room-temperature ($T\approx 300$ K and below) x-ray[25] and neutron-diffraction[26,27] studies show that the HSQ crystal is monoclinic with a structure built up from pseudosymmetric hydrogen-bonded layers (Fig. 1). Consequently for $T>T_{cH}$, the hydrogen atoms are asymmetrically disposed in the O—H $\cdots$ O bonds. The HSQ molecules are joined together to form infinite sheets by means of ordered asymmetric H bonds in the crystallographic mirror plane with lattice constants $a=6.143$ Å, $b=3.286$ Å, $c=6.148$ Å, $\beta=89.96°$, and $Z=2$. As shown in Fig. 2 the molecules in one layer are related to those above and below by the twofold screw axis. The individual layers thus constitute ferroelectrically ordered sublattices which are antiferroelectrically stacked in a pseudotetragonal body-centered fashion. The coupling between the layers (separated by $b/2=2.636$ Å), i.e., the interlayer coupling, is weak, whereas strong interaction between the different hydrogen bonds is transmitted via the C_4O_4 skeleton by a movable double bond within each layer. This two-dimensional structure is therefore expected to play a dominant role in the mechanism of SPT as observed by Semmingsen[26] and Semmingsen and Feder[2] from the neutron scattering and optical birefringence experiments.

The high-temperature structure ($T>T_{cH}$) of HSQ is indeed very similar to the low-temperature ($T<T_{cH}$) monoclinic phase. The HSQ molecules are joined by H bonds running along [101] to form planar layers perpendicular to the b axis. The H-bond arrangement within a

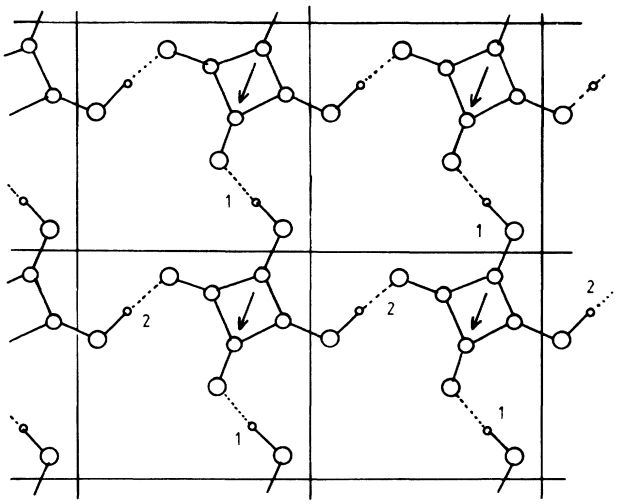

FIG. 2. One layer of squaric acid (HSQ) with the vector sum of 2-hydrogen displacements indicated at the center of the C_4O_4 unit to which they belong (Refs. 6 and 9).

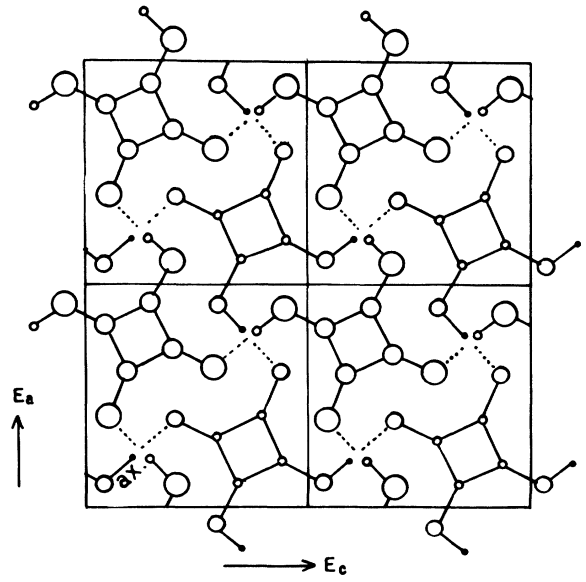

FIG. 3. The structure of squaric acid at room temperature. The unique axis is vertical. Two molecular layers are shown. Large circles: oxygen; intermediate circles: carbon; and small circles: hydrogen. The hydrogen bonds are indicated by dotted lines (Refs. 6 and 9).

layer is relatively open; however, the neighboring layers related to body centering of the lattice are fitted into the open areas to produce a very dense stacking along the b axis. The protons are thus distributed equally over both sites in the H bonds. The individual layers, therefore, carry no spontaneous polarization, P_s. This situation seems to be very similar to the case of the quasi-one-dimensional $PbHPO_4$ crystal where the pseudospin-lattice coupled-mode (PLCM) model was previously applied by us.[16]

Our organization of the paper is as follows. In Sec. II we set up the four-sublattice cluster Hamiltonian in accordance with the H-bond structure of HSQ. Calculations of electrical susceptibility and transition temperature have been made in Sec. III. In Sec. IV the derived theoretical expressions have been fitted with the available experimental data of dielectric constants. Analysis of various salient features of HSQ as discussed in Sec. I has also been made in this section. Finally, the paper ends with a short summary and conclusion suggesting the existence of a "crossover" phenomenon in this crystal and the unified character of the PLCM model for the explanation of SPT in the H-bonded HSQ and in other systems.

II. THE PSEUDOSPIN MODEL

In Fig. 3 the four unit cells of HSQ projected on the (010) is shown. The H bond is surrounded by six nearest-neighbor bonds. Four of these bonds are in the ac plane including the given bond, while each of the other two bonds is in the plane just above and below the given bond. Following Yasuda *et al.*[9] each bond along the a axis may be distinguished from each other by assuming the presence of $+a$ and $-a$ bonds. There is an antiferroelectric arrangement of the $+a$ and $-a$ bonds within the ac plane, consequently the bond interaction parameter between the ac plane (say, K) is expected to be weaker than that within the ac plane (say, J). Similarly, along the c axis each bond is distinguished from each other as the $+c$ and $-c$) bonds as shown in Fig. 2.

From the consideration of the H-bond arrangements (Fig. 2) it also appears that a theoretical treatment of antiferroelectric HSQ based on a pseudospin model Hamiltonian should incorporate both the transverse long-range dipole-dipole antiferroelectric interaction and the interaction between the transverse dipole and an external field. In order to include transverse properties we take into account the changes in transverse dipole moments induced by the field acting on the protonic displacements along the H bonds. Thus one could distinguish between two kinds of hydrogen bonds in HSQ. The bond labeled plus (or minus) contributes positively (or negatively) to polarization along the $a(b)$ or c direction. This concept has also been used by Yasuda *et al.*[9] to explain the pressure-dependent dielectric constant of HSQ. They also concluded that the model used for the explanation of antiferroelectric (AFE) character of ADP crystal might also be applicable to squaric acid crystal. However, there are also differences in the arrangements of H bonds in the lattices of ADP and HSQ which are quite evident from the structural differences between these two crystals.

Considering the above picture of the H-bond arrangements in HSQ, the polarizations along the $a(b)$ and (c) directions may be written as

$$P_b \propto \left[\sum_i Z_i^{+a} - \sum_i Z_i^{-a}\right] \quad \text{and} \quad P_c \propto \left[\sum_i Z_i^{+c} - \sum_i Z_i^{-c}\right], \tag{2}$$

respectively, where $Z^{\pm m}$ is the component of the pseu-

dospin operator with a plus or minus bond aligned in the m direction (where m is either a or c). The bonds along each direction are divided again into two sublattices designated by (1) and (2), so that alternating layers belong to different sublattices as shown in Fig. 2. We also include in this Hamiltonian an antiferroelectric long-range interaction (λ) between the dipoles of the two different sublattices in each direction. Thus the proposed pseudospin Hamiltonian in the four-sublattice-cluster approximation[11] can be written as

$$H_1=-\Omega\sum_i X_i-\tfrac{1}{2}\sum_{i,j}J_{ij}Z_iZ_j-(\mu_cE_c+K\langle Z\rangle)\sum_i Z_i$$
$$-\sum_{m=a,b}[\mu_mE_m-\tfrac{1}{2}\lambda\langle Z^{+m}(2)-Z^{-m}(2)\rangle]\left[\sum_i Z_i^{+m}(1)-\sum_i Z_i^{-m}(1)\right]$$
$$-\sum_{m=a,c}[\mu_mE_m-\tfrac{1}{2}\lambda\langle Z^{+m}(1)-Z^{-m}(1)\rangle]\left[\sum_i Z_i^{+m}(2)-\sum_i Z_i^{-m}(2)\right]. \tag{3}$$

The first part of this Hamiltonian represents the effective short-range proton-proton interaction and is the same as the usual Blinc–de Gennes Hamiltonian [Eq. (1)] for the KDP-type crystals with Ω as the effective tunneling frequency. The second part represents the interaction of the spins with an external field (E_c) along the c direction and their interaction with the average longitudinal polarization $\langle Z\rangle$ via the long-range dipole interaction (K). The last part is the long-range antiferroelectric interaction term. The dipole moment along the m axis is denoted by μ_m ($m=a,b,c$).

Since the solution of th pseudospin model for both the KDP-and ADP-type crystals with a four-sublattice-cluster approximation adequately describes most of the static properties of these crystals,[11,28,29] we apply this approximation to the Hamiltonian in Eq. (1) for HSQ.

Now if one defines quantities like Z_1 and Z_3 as the Ising pseudospins representing the minus and plus H bonds along the a direction (pseudospin at $y=\frac{1}{4}$), and Z_2 are those for the b direction (pseudospin at $y=\frac{3}{4}$) as shown in Fig. 2, the one-particle Hamiltonian for the plus and minus bonds aligned along the a direction is given by (neglecting, for the time being, the tunneling term)

$$H^{+a}(1)=[\mu_1E_c+K\langle Z\rangle+\rho_c+\mu_2E_a-\tfrac{1}{2}\lambda\langle Z_3(2)-Z_1(2)\rangle+\rho_a]Z_3(1), \tag{4}$$
$$H^{-a}(1)=-[\mu_1E_c+K\langle Z\rangle+\rho_a-\mu_2E_a+\tfrac{1}{2}\lambda\langle Z_3(2)-Z_1(2)\rangle-\rho_a]Z_1(1). \tag{5}$$

Similarly one can write the one-particle Hamiltonian for the bonds along the c direction. The parameters ρ_a, ρ_b, and ρ_c are, respectively, the energies due to the effective fields along the a, b, and c directions, produced by the adjacent bonds outside the cluster. μ_a and μ_2 are the dipole moments along the $a(b)$ and c directions, respectively.

The Hamiltonian for the pseudospins belonging to the second sublattice, viz., $H^{\pm a}(2)$ has also the same form as described by Eqs. (2) and (3). The effective cluster fields ρ_a, ρ_b, and ρ_c follow the cluster equilibrium condition, viz.,

$$\frac{\partial F}{\partial\rho_a}=\frac{\partial F}{\partial\rho_b}=\frac{\partial F}{\partial\rho_c}=0, \tag{6}$$

where F is the approximate Helmholtz free energy given by

$$F=-\frac{1}{2\beta}\left[\ln\bar{Z}_4(1)+\ln\bar{Z}_4(2)-\tfrac{1}{4}\sum_{\substack{n=1,2\\m=a,b}}\ln\bar{Z}^{+m}(n)+\ln\bar{Z}^{-m}(n)\right]+K\langle Z\rangle^2$$
$$+\tfrac{1}{4}\lambda\sum_{m=a,b}\langle Z^{+m}(1)-Z^{-m}(1)\rangle\langle Z^{+m}(2)-Z^{-m}(2)\rangle, \tag{7}$$

where $\beta=1/k_BT$ (k_B is Boltzmann's constant and T is the absolute temperature) and $\bar{Z}_4(n)$ is the partition function of the four-particle Hamiltonian. The four- and one-particle Hamiltonian $H_4(n)$ and $H^{\pm m}(n)$, respectively, describing the energy of four pseudospins associated with four hydrogen bonds in which all the pseudospins belong to sublattice (1), can be written as

$$H_4(1)=-V[Z_1(1)Z_2(1)+Z_2(1)Z_3(1)+Z_3(1)Z_4(1)+Z_4(1)Z_1(1)]-U[Z_1(1)Z_3(1)+Z_2(1)Z_4(1)]$$
$$-(\mu_1E_c+K\langle Z\rangle+\tfrac{1}{2}\rho_c)\sum_{n=1}^{4}Z_n(1)-[\mu_1E_c-\tfrac{1}{2}\lambda\langle Z^{+a}(2)-Z^{-a}(2)\rangle+\tfrac{1}{2}\rho_c][Z_3(1)-Z_1(1)]$$
$$-[\mu_2E_b-\tfrac{1}{2}\lambda\langle Z^{+b}(2)-Z^{-b}(2)\rangle+\tfrac{1}{2}\rho_b][Z_2(1)-Z_4(1)]-\Omega\sum_{n=1}^{4}X_n(1), \tag{8}$$

where U and V are the short-range interaction energies related to the Slater-Takagi parameters[28] ε_1 and ε_0 ($4U=-2\varepsilon_1+2\varepsilon_0$ and $4V=2\varepsilon_1-\varepsilon_0$). Similar expression as in Eq. (8) also hold for the Hamiltonian $H_4(2)$. The three-proton configuration energy ε_1 appears to be very large for HSQ as there is a large discontinuity in the χ_a versus T curve at the transition temperature.[7] Therefore the transition temperature T_c is calculated from the free energy F using the standard procedure and then one obtains

$$\exp(-\lambda/k_B T_c)=\alpha/[2+\exp(\varepsilon_0/k_B T_c)] , \tag{9}$$

where α is a numerical constant factor to be evaluated from fitting of the experimental data. Equation (9) is also true for the antiferroelectric ADP-type crystals.

III. THEORY

A. Green's-function method

It should be mentioned here that the pure pseudospin Hamiltonian containing the tunneling term considered in our subsequent calculations with Green's-function technique[30,31] has the general form

$$H_2=-2\Omega\left[\sum_i X_i+\sum_{m=a,b}\sum_{n=1,2}J_{ij}Z_i^{+m}(n)Z_i^{-m}(n)\right] . \tag{10}$$

It has also been mentioned in Sec. I that for the HSQ crystal the proton lattice interaction is expected to be quite large and therefore we also introduce a linear pseudospin-phonon coupling term which in its simplest form can be written as

$$\begin{aligned}H_3=&N^{-1/2}\sum_{i,q}V_{iq}Q_q Z_i \\ &-N^{-1/2}\sum_{m=a,b}\sum_{n=1,2}\sum_{i,q}V_{iq}Z_i^{+m}(n)-Z_i^{-m}(n)Q_q \\ &+\tfrac{1}{2}\sum_{q,-q}(P_q P_{-q}+\omega^2 Q_q Q_{-q}) .\end{aligned} \tag{11}$$

For the overdamped system like HSQ one may replace $\sum\omega^2 Q_q Q_{-q}$ by a complex frequency $\omega_q=(\omega-i/\tau_q)Q_q Q_{-q}$ (where τ_q is the relaxation time). In Eq. (11) $V_{i,q}$ is the usual spin-phonon coupling term, Q_q and P_q are, respectively, the normal coordinates and conjugate momenta. To simplify our calculations we further assume that $V_{i,q}^{\pm m}=V_{i,q}$, $Q_q^{\pm m}=Q_q$, and $P_q^{\pm m}=P_q$ and hence the present model could be treated as a modified Kobayashi model.[32]

For the antiferroelectric transition in HSQ, where the instability is assumed to occur at the zone boundary, the order parameter $\langle Q_{q_0}\rangle=0$; and one has

$$\begin{aligned}&\langle Q_l\rangle=Q_{q_0}\exp(iq_0R_1)\approx\pm Q_{q_0} , \\ &Q_q=Q_{q_0}+\delta Q_q .\end{aligned} \tag{12}$$

In the paraelectric phase (PE) $Q_q=0$ and $\delta Q=Q_q$ (say) denotes the fluctuations around the average value.

B. Calculation of electrical susceptibility

To calculate the static electrical susceptibility along a and c directions, we use the generalized Hamiltonian (10). It has already been mentioned in our earlier papers[13–16] that the double time-temperature–dependent Green's function[30] has the generalized form

$$G^{+m,n}(t-t')=\langle\langle S_i^{m,n}(t)|S_j^{m,n}(t')\rangle\rangle , \tag{13}$$

where $S=X,Y,Z$ are the components of the pseudospin variables. The Fourier transform of Eq. (13) has the form

$$\begin{aligned}\varepsilon\langle\langle S_i^{m,n}|S_j^{m,n}\rangle\rangle=&(2\pi)^{-1}\langle[S_i^{m,n},S_j^{m,n}]\rangle \\ &+\langle\langle[S_i^{m,n},H]|S_j^{m,n}\rangle\rangle ,\end{aligned} \tag{14}$$

where $\langle\ \rangle$ denotes as before the statistical average of the enclosed pseudospin operators. By using the Green's-function theory, as used, one has calculated first the correlation function from which the required physical parameters could be calculated. The corresponding correlation functions[13] of the two operators, viz. $\langle S_i^{\pm m,n}S_j^{\pm mn,}\rangle$ necessary to evaluate for our calculations are obtained from the spectral theorem, viz.,

$$\langle S_{i(n)}^{+m}|S_{j(n)}^{+m}\rangle=i\lim_{\delta\to0}\int_{-\infty}^{+\infty}\frac{N}{L}R\,d\epsilon , \tag{15}$$

where

$$N=\langle\langle S_i^{\pm m}(n)|S_j^{\pm m}(n)\rangle\rangle_{\epsilon+i\delta}-\langle\langle S_i^{\pm m}(n)|S_j^{\pm m}(n)\rangle\rangle_{\epsilon-i\delta}$$

and $L=[\exp(\beta\epsilon)-1]$ and $R=e^{-i\epsilon(t-t')}$. For different components of S, Eq. (14) gives nine different coupled equation like $\langle\langle X_i^{\pm m}(n)Y_j^{\pm m}(n)|Z_i^{\pm m}(n)\rangle\rangle$, etc. To calculate the individual two-particle Green's-function from these coupled Green's functions we linearize the higher-order Green's functions using the random-phase approximation (RPA) of Bogolyubov and Tyablikov.[13,31] For example, three of the total nine such linearized equations of motion obtained from Eq. (14) can be written in the form

$$\begin{aligned}&\begin{bmatrix}E & W & 0\\ W & E & 0\\ 0 & 0 & E\end{bmatrix}\begin{bmatrix}1 & 0 & 0\\ 0 & 1 & 0\\ 0 & 0 & 1\end{bmatrix}\begin{bmatrix}G^{+m,n}(XX)\\ G^{+m,n}(YX)\\ G^{+m,n}(ZX)\end{bmatrix} \\ &\qquad=\frac{i}{2\pi}\begin{bmatrix}0\\ -Z^{+m}(n)\\ Z^{+m}(n)\end{bmatrix} ,\end{aligned} \tag{16}$$

where $G^{m,n}(XX)=\langle\langle X_i^m(n)|X_j^m(n)\rangle\rangle$ and so on,

$$W=i\lambda'-i\mu_a E_a ,$$

$$\lambda'=\lambda[\langle Z^{+m}(n)-Z^{-m}(n)\rangle] .$$

$G^{+m,n}(XX)$, $G^{+m,n}(YX)$, $G^{+m,n}(ZX)$, etc. are the Green's functions, like that represented by Eq. (13). Solving Eq. (16) for all the Green's function like $G^{\pm m,n}(ZZ)$ and then using Eq. (15) we get the required correlation functions like $\langle Z^{\pm m}(n)Z^{\pm m}(n)\rangle$, etc. Next we assume that all the correlation functions are finite and obey the identity of the form

$$\langle X^2\rangle+\langle Y^2\rangle+\langle Z^2\rangle=S(S+1)=\text{const}=\Phi . \tag{17}$$

This constant has to be obtained from fitting of the experimental data.

Using Eq. (16) and the correlation functions $\langle Z^{\pm m}(n)Z^{\pm m}(n)\rangle$ we find (following the procedure of our earlier paper[13]) for sublattice (1) and sublattice (2) in the $\pm a$ direction

$$\langle Z^{\pm a}(1)\rangle = \mp\Phi\tanh\beta\frac{(\lambda'-\mu_a E_a)}{2}, \tag{17a}$$

$$\langle Z^{\pm a}(2)\rangle = \mp\Phi\tanh\beta\frac{(\lambda''-\mu_a E_a)}{2}, \tag{17b}$$

where $\lambda''=\lambda[\langle Z^{+a}(n=1)\rangle-\langle Z^{-a}(n=1)\rangle]$. The sublattice polarization along the $a(c)$ direction is given by

$$P_a=\langle Z^{+a}(1)\rangle+\langle Z^{+a}(2)\rangle-\langle Z^{-a}(1)\rangle-\langle Z^{-a}(2)\rangle . \tag{18}$$

From (18) the electrical susceptibility χ_a comes out to be

$$\chi_a=\left[\frac{\partial P_a}{\partial E_a}\right]_{E_a=0}N_a\mu_a$$
$$=\Phi\frac{N\mu^2 a}{k_BT}\left[2-\left[\tanh^2\frac{\lambda'}{2k_BT}+\tanh^2\frac{\lambda''}{2k_BT}\right]\right] . \tag{19}$$

Now putting

$$\langle Z^{+m}(1)\rangle-\langle Z^{-m}(1)\rangle=\langle Z^{+m}(2)\rangle-\langle Z^{-m}(2)\rangle=2 \tag{20}$$

for the AFE phase transition in HSQ we get

$$\chi_a=\frac{2\Phi}{k_BT}N_a\mu_a^2\left[1-\tanh^2\frac{\lambda^2}{k_BT}\right] . \tag{21}$$

Equation (21) can be used to study the electrical field dependence of electrical susceptibility and hence dielectric constant ($\epsilon_a\simeq 1+4\pi\chi_a$). This is the general relation to calculate the static dielectric constant without considering the pseudospin-phonon interaction which we consider to be important. This equation cannot, however, be used to show the dome-shaped dielectric constant above T_c.

To consider the effect of pseudospin-lattice interaction one has to deal with the generalized Hamiltonian of the form

$$H\equiv H_1+H_2+H_3 . \tag{22}$$

Again calculating all the required Green's functions like $G^{+m,n}(SS)=\langle\langle S^{\pm m}(n)|S'^{\pm m}(n)\rangle\rangle$, etc. and applying the procedure discussed above we find the susceptibility along the a axis

$$\chi_a(q=0)=\left[\frac{\partial P_a}{\partial E_a}\right]_{E_a=0}=\frac{N_a\mu_a^2}{k_BT}[\chi_a] , \tag{23}$$

where

$$\chi_a=\frac{\theta_1^2}{(\theta_1^2+4\Omega^2)}+\frac{\theta_2^2}{(\theta_2^2+4\Omega^2)}+\frac{\tanh[\frac{1}{2}\beta(\theta_1^2+4\Omega^2)^{1/2}]}{(\theta_1^2+4\Omega^2)}\left[\frac{8\Omega^2k_BT}{(\theta_1^2+4\Omega^2)^{1/2}}-\theta_1^2\tanh[\tfrac{1}{2}\beta(\theta_1^2+4\Omega^2)^{1/2}]\right]$$
$$+\frac{\tanh[\frac{1}{2}\beta(\theta_2^2+4\Omega^2)^{1/2}]}{(\theta_2^2+4\Omega^2)}\left[\frac{8\Omega^2k_BT}{(\theta_2^2+4\Omega^2)}-\theta_2^2\tanh[\tfrac{1}{2}\beta(\theta_2^2+4\Omega^2)^{1/2}]\right] , \tag{24}$$

where $\theta_1^2=\lambda'-\bar{V}_0$, $\theta_2^2=\lambda''-\bar{V}_0$, and $\bar{V}_0=V_{q_0}\langle Q_{q_0}\rangle$. The corresponding electrical susceptibility along the c axis has the form

$$\chi_c=\left[\frac{\partial P_c}{\partial E}\right]=\frac{N_c\mu_c}{2k_BT}(\chi_c) ,$$

where

$$\chi_c=\frac{\theta_1'^2}{(\theta_1'^2+4\Omega^2)}+\frac{\tanh[\frac{1}{2}\beta(\theta_1'^2+4\Omega^2)^{1/2}]}{(\theta_1'^2+4\Omega^2)}\left[\frac{8\Omega^2k_BT}{(\theta_1'^2+4\Omega^2)}-\theta_1'^2\tanh[\tfrac{1}{2}\beta(\theta_1'^2+4\Omega^2)^{1/2}]\right] ,$$

where

$$\theta_1'^2=(J_0'+\gamma+\bar{V}_0)\langle Z\rangle$$

and

$$J_0'=\sum_{j'}J_{ij},\quad \langle Z\rangle=\left[\frac{1}{2N}\right]\sum_{i=1}^{N}(Z_i) . \tag{25}$$

This Eq. (25) is also valid for the KDP-type crystal for χ along the polarization axis. The longitudinal polarization has been defined as $P_c=N_c\mu_c\langle Z\rangle$. Here we have for the ferroelectric phase $Z=1$ and for the antiferroelectric phase Eq. (20) is valid. The expressions for χ_a and χ_c appear to be identical with those derived for the ADP-type crystals.[29] This is evident from the similar nature of the model Hamiltonians used for ADP and HSG.

IV. RESULTS AND DISCUSSION

As mentioned in Sec. I, one of the purposes of our present investigation is to describe the anomalous

TABLE I. The pseudospin-lattice coupled-mode (PLCM) model parameters for HSQ obtained from best fitting of the experimental data of dielectric constant at different temperature and fixed pressure. The value of α [Eq. (9)] is taken to be 2 for HSQ.

Sample	Pressure (GPa)	$\bar{\Omega}$ (cm^{-1})	λ/k_BT	$\bar{V}_0/k_BT_c$	$8N\mu^2$ (esu)	B	J_0^* (cm^{-1})	T_c (K)	ε_0/k_B
HSQ	0.60	14	300.80	67.58	2820	0.012	530	310	368.00
	0.45	15	338.75	98.05	2680	0.021	550	326	422.40
	0.15	20	387.50	100.80	2580	0.022	580	360	486.00
	0.00	18	438.50	85.80	2600	0.020	611	374	510.00

thermal and pressure dependencies of dielectric constants of both HSQ and DSQ using Eq. (21) for the electrical susceptibility along the a axis. It is well known that the standard relation for the transition temperature has the general form[33]

$$\tanh(\Omega/k_BT_c)=\Omega/J^* , \tag{26}$$

where J^* is the effective exchange interaction. Equation (26) is also qualitatively valid for squaric acid.[7] An estimate of the approximate values of the model parameters Ω and J^* is obtained first from this equation. By putting the approximate values of $\bar{V}_0$, J^*, and χ_a in the expression for χ_a, the experimental ($\chi_a - T$) curves for different pressure parameters $p=0$, 0.15, 0.45, and 0.60 GPa are fitted (by a trial and error method). The model parameters for the best fitting are shown in Table I. The increase of dielectric constant with temperature in the paraelectric phase is explained by assuming that the moment $N\mu_a$ has two parts: (a) a temperature-independent part and (b) a temperature-dependent part, i.e., by writing

$$N\mu_a=[1+B(T-T_c)] , \tag{27}$$

This is assumed because of the fact that with increase of temperature the effective separation between the charges of the dipoles increases, resulting in an increase in $N\mu_a^2$ values. The parameter "B" is treated as a new parameter (shown in Table I). It is also found that the number of dipole moments N increases by 0.3%/kbar because the volume compressibility is $d\ln V/dp \approx 0.3\%$/kbar. Since Ω is very small, the effect of pressure on Ω is neglected. The AFE interaction between the bonds (λ) is found to decrease with pressure (see Table I). The value of $d\ln\mu/dp \approx -2\%$/kbar is much larger than the value of the linear compressibility.[9] Therefore it is expected that the value of λ should decrease with pressure.

The model parameters calculated for DSQ from fitting the experimental dielectric constant ϵ_a' versus temperature curves with different pressures are shown in Table II. While fitting the experimental data (both for HSQ and DSQ) in the low-temperature region (below T_c) we used the relation

$$\langle Z\rangle=[1-(T/T_c)]^{0.14} \tag{28}$$

as given by the neutron scattering theory.[17]

It is observed both from Tables I and II that the values of λ and $\bar{V}_0$ are very much sensitive to pressure (Ω is assumed to be zero for the deuterated DSQ salt). The appreciable magnitude of $\bar{V}_0$ indicates the importance of proton-lattice interaction in squaric acid which was, however, neglected in the calculations of previous authors.[2,3,8,27] The ϵ_a' versus T curves (both theoretical and experimental) at different pressure as shown in Figs. 4 and 5 indicate reasonably good agreement.

Using Eq. (9) and the parameters from Tables I and II, the values of ε_0/k_B come out to be of the order of 486, 422, and 368 K, respectively, at 0.15, 0.45, and 0.60 GPa for HSQ. The corresponding values of (ε_0/k_B) for DSQ are 530, 474, 452, and 440 K, respectively, for 0.20, 0.60, 1.20, and 1.80 GPa. Therefore the values of Slater energy ε_0 decreases with pressure which is similar to the variation of long-range antiferroelectric interaction parameter λ. It is found that the round-shaped dielectric constant around T_c cannot be clearly explained without changing the model parameters as shown in Tables I and II. This might be due to critical fluctuations around T_c. However, changing the values of the parameters λ, V_0, and Ω by about 5–10% the round nature of the ($\epsilon_a' - T$) curve around T_c can be fitted with the present pseudospin-lattice coupled-mode model. This change of the model parameters might also be justified from the fact that the critical region is a fluctuating region. For a similar variation ($\sim$10%) of the model parameters for fitting the

TABLE II. The pseudospin-lattice coupled-mode (PLCM) model parameters for DSQ obtained from best fitting of the experimental data of dielectric constant at different temperature and fixed pressure. The value of α [Eq. (9)] is taken to be 2 for DSQ.

Sample	Pressure (GPa)	$\bar{\Omega}$ (cm^{-1})	λ/k_BT	$\bar{V}_0/k_BT_c$	$8N\mu^2$ (esu)	B	J_0^* (cm^{-1})	T_c (K)	ε_0/k_B
DSQ	1.80	60	358.55	150.00	3512	0.017	518	385	432.47
	1.20	50	379.80	158.90	3655	0.018	555	415	440.10
	0.60	40	390.00	165.80	3855	0.020	580	460	451.60
	0.40	50	409.50	169.00	4005	0.022	610	482	473.81
	0.20	50	448.00	180.50	4136	0.022	660	505	530.00

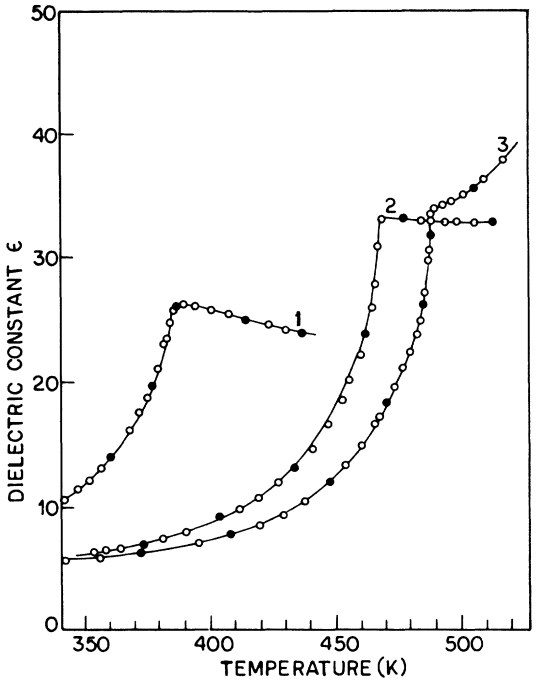

FIG. 4. Thermal variations of dielectric constants of squaric acid (HSQ) at different fixed pressures: (1) 0.66 GPa, (2) 0.45 GPa, and (3) 0.15 GPa [○, experimental (Ref. 7) points; —·—·—·, theoretical curve].

transverse susceptibility of the KDP crystal we find $T_{\max}/T_c \approx 1.09$ which agrees with the values shown by Samara and Semmingsen.[7] For this variation of the model parameters the ratio $T_{\max}/T_c$ does not exceed 1.03 for HSQ and 1.015 for DSQ which agrees with the values

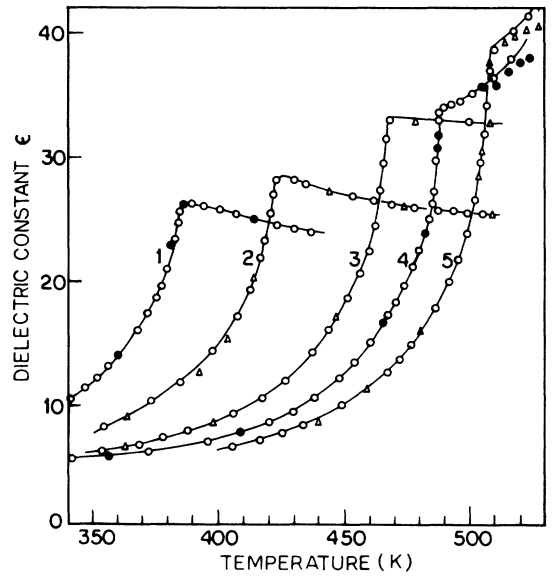

FIG. 5. Thermal variations of dielectric constants of deuterated squaric acid (DSQ) at different fixed pressures: (1) 0.20 GPa, (2) 0.40 GPa, (3) 0.60 GPa, (4) 1.20 GPa, (5) 1.80 GPa [○, experimental (Ref. 7) points; △,●, theoretical points].

(1.02 and 1.013, respectively) obtained experimentally.[7]

The round-shaped susceptibility curve around T_c of HSQ resembles that of the KDP crystal observed along the transverse axis.[22] Similar behavior is also observed for the antiferroelectric phase transition in ADP crystal. It therefore appears that the dielectric properties of all these crystals could be studied with a single unified Hamiltonian. It is most probable that this type of pseudospin model could be applied even for the case of 1D antiferroelectrics, Jahn-Teller crystals like $PrCl_3$,[23] and antiferroelectric $KMnF_3$ (Ref. 7) showing similar maxima in the $(\epsilon_a' - T)$ curve above T_c. This features also resembles the behavior of antiferromagnetic susceptibility.[7] To find if Fisher's explanation[34,27] of the above maximum (in case of an antiferromagnet) is even applicable to the present AFE case, we calculate the mean value of specific heat C from the relation

$$\bar{C}(T) \simeq A \frac{\partial}{\partial T}[T\chi_a(T)] . \tag{29}$$

The expression for the susceptibility $\chi_a(T)$ is differentiated with respect to T and the values of $\bar{C}(T)$ are calculated from the values of the model parameters obtained from fitting the experimental dielectric-constant curves (see Tables I and II). Though the parameter A is a merely temperature-dependent term, we consider it to be constant. Our interest is to find whether a λ-type anomaly in specific heat versus temperature curve should be exhibited by HSQ as was pointed out by Feder.[3] Using Eq. (29) a λ-type anomaly in $\bar{C}$ is actually found in the $\bar{C}$ versus T curve near the antiferroelectric transition when $\partial\chi_a/\partial T \to \infty$ at T_c. Figure 7 shows $\bar{C}/A$ versus T curve calculated for HSQ by using the model parameters from Table I for 0.15 GPa. From Fig. 6 we find that the maximum peak for HSQ appears at about 7 K above T_{cH} which is very close to the value ~ 7.5 K observed by Samara and Semmingsen.[7] The heat-capacity anomaly also appears to be of the λ type. This finding definitely supports our theoretical calculations with pseudospin-lattice coupled-mode model applied for HSQ and DSQ.

The maximum in ϵ_a' above T_c then follows from the requirement that ϵ_a' ultimately tends to zero at high temperature because of the loss of pseudospin correlations. This is a very interesting result in the case of an antiferroelectric material like HSQ showing good analogy with antiferromagnets, and more generally it is expected that the arguments made by Fisher[34] for AFM are physically significant. Equation (29) should therefore be qualitatively valid even for the AFE squaric acid earlier suggested by Feder.[3]

Another feature of equal importance which needs further clarification is the crossover between first- and second-order transition recently concluded from the chemical shift measurement by Mehring and Becker.[35] To make a test of this interesting feature we made the following phenomenological approach.

It is observed from the studies of the experimental data of specific heat (ΔC),[36,37] optical birefringence (Δn_{bc}),[2] chemical shift $(\Delta\sigma)$,[18] and the temperature dependence of the elastic constant (C_{11}),[38] that these parameters behave similarly near the phase transition. That is, one

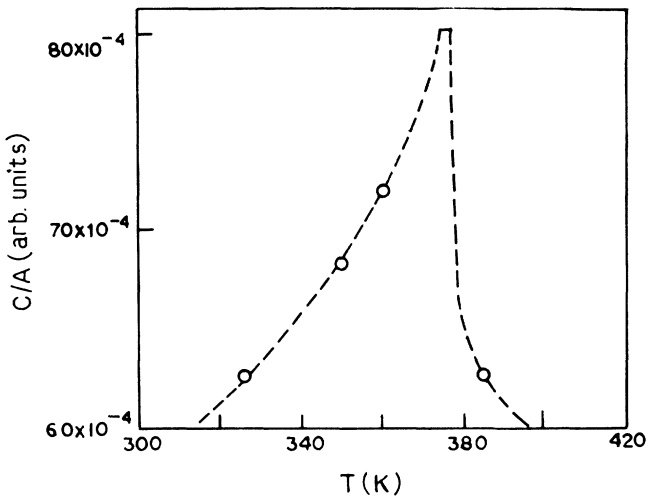

FIG. 6. Calculated specific heat of HSQ using the model parameters (for $p=0$) from Table I.

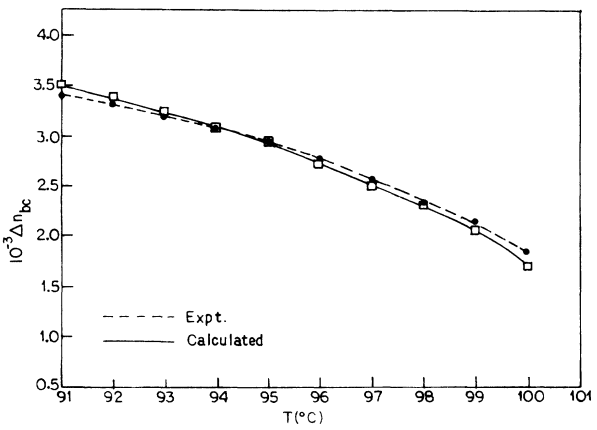

FIG. 7. Thermal variation of birefringence of squaric acid (HSQ) (Ref. 20).

such parameter could be mapped into the other by a constant scaling factor. To see whether the transition is first or second order, critical analysis of any of these parameters would be interesting. We have tried to study the refractive-index change (Δn_{bc} of HSQ in the light of our theoretical model. From the variation of Δn_{bc} the order of the transition could be detected in the following manner.

The free-energy density for squaric acid can be expressed as

$$F=\tfrac{1}{2}a'(T-T_0)Q^2+\tfrac{1}{4}bQ^4+\tfrac{1}{6}cQ^6 , \tag{30}$$

where T_0 is the temperature of the stability limit for the prototype phase. Here we assume a linear variation of Δn_{bc} with Q^2 (square of the order parameter). The temperature dependence of the elastic function C_{11} as derived from the velocity measurement[38] also supports this assumption.[5]

If we consider that birefringence is a direct measure of the spontaneous strain (e^s) through an "internal" elasto-optic effect,[39] a linear relationship between Δn_{bc} and spontaneous strain is expected. This implies that Δn_{bc} should also be proportional to Q^2, and so measurement of Δn_{bc} as a function of T can prove the behavior of the order parameter. A good set of experimental data of birefringence is expected to give a more accurate impression for the order-parameter behavior than other experimental data which directly give either e^s or Q.

Since $\Delta n_{bc} \propto Q^2$, the observed linear dependence of $(\Delta n_{bc})^2$ on T implies that the critical exponent β in the expression $Q \propto (T_0-T)$ has a value (~ 0.25 for $T<366$ K). This indicates that below 366 K the behavior is determined by a tricritical fixed point,[40,41] where $b=0$ in Eq. (30). At the transition temperature T_c, however, a first-order behavior ($b<0$) is expected and Fig. 5 suggests a crossover from a tricritical region to a first-order region at about 366 K, the first-order region being in a reduced temperature range of ~ 0.05. Similar behavior has also been revealed from the linear separation ($\Delta\sigma$) in the high-resolution ^{13}C NMR spectra[18,19] (chemical-shift measurement), and also from birefringence measurements.[2] The evidence of a crossover phenomenon in HSQ is, therefore, quite strong and demands further new experimental results.

The high-pressure studies of the dielectric properties by Samara and Semmingsen[7] and others,[9,40] however, did not mention the tricritical nature of the transition in HSQ. The application of high pressure to squaric acid may decrease the first-order regime so that a true tricritical point becomes hard to detect.

Let us now consider the first-order region between 360 K and T_c in more detail. If the system is described within the mean-field approximation, the order parameter should have the following temperature dependence.[42]

$$Q^2(T)=\tfrac{2}{3}(\Delta Q_0)^2\left\{1+\left[1-\frac{3}{4}\left[\frac{T-T_0}{T_c-T_0}\right]\right]^{1/2}\right\} , \tag{31}$$

where ΔQ_0 is the jump in the order parameter at the

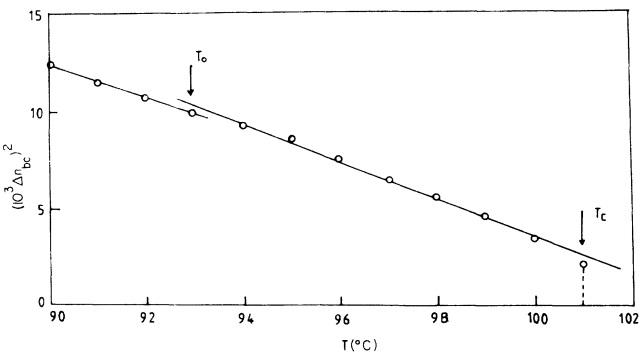

FIG. 8. Thermal variation of $(\Delta n_{bc})^2$ of squaric acid (HSQ) showing the anomaly at $T_0 > T_c$ (theoretical curve).

first-order transition occurring at temperature T_c. Since $\Delta n_{bc} \sim Q^2$, the same temperature variation is to be expected for Δn_{bc}, such that one could write

$$n_{bc}(T)=\tfrac{2}{3}(\Delta n_{bc}^0)\left\{1+\left[1-\frac{3}{4}\left[\frac{T-T_0}{T_c-T_0}\right]\right]^{1/2}\right\}. \quad (32)$$

Using (31) a least-squares fit of the data points between 366 and 375 K gives the solid curve shown in Fig. 7 and 8. In this least-squares refinement T_c was kept fixed at the experimentally observed value of 375 K and the two parameters, viz., T_0 and n_{bc}^0, were fitted to several data points. The best fit was obtained for $T_0=373.49(\pm 2)$ K and $n_{bc}^0=(1.50\pm 0.05)\times 10^{-3}$ also obtained by Kuhn *et al.*[20] Though the transition temperature T_c is sensitive to the pressure and the presence of impurities, the difference $T_c-T_0=(373.49\text{ K}-366\text{ K})=7.49$ K obtained from our calculations is comparable to the value of 7 K obtained by Samara and Semmingsen.[7]

V. SUMMARY AND CONCLUSION

Squaric acid is an interesting quasi-two-dimensional antiferroelectric crystal. A four-sublattice-cluster Hamiltonian has been found to be suitable for investigating the first-order nature of the transition observed in this crystal. Using the pseudospin-lattice coupled-mode model we have shown that the tunneling term is extremely small for this salt compared to the other H-bonded KDP crystals. But its contribution cannot be neglected. The pseudospin-phonon interaction is also quite important for the HSQ crystal as observed from the values of the pseudospin-phonon interaction parameter $\bar{V}_0$. This is also supported from the very high value of $k_B T_c$ in HSQ (indicating the importance of phonons in the transition mechanism).

The cluster pseudospin Hamiltonian used in this paper is found to be adequate to explain most of the salient features of the antiferroelectric first-order transition in HSQ and DSQ. There is very close similarity between the model Hamiltonian used for HSQ and that used for ADP crystal which was also pointed out by Yasuda *et al.*[9] This means that basically the pseudospin models describing the transverse dielectric constant of KDP, and the antiferroelectric behavior of ADP, and HSQ are similar in their forms. That is, a unified PLCM-type model could be used for the studies of various physical properties of these crystals with different sets of model parameters varying from crystal to crystal.

The rounding of the $\epsilon_a' - T$ curve about T_c which is a characteristic feature of HSQ salt is actually found to be due to a large order-parameter fluctuation as also suggested by Petersson and Maier.[5] It is also pointed out from our calculations that the dome-shaped nature of the $\epsilon_a' - T$ curve above T_c could be fitted with the theory considering small fluctuations of the pseudospin model parameters which are also related to the order-parameter fluctuations. Here it might also be concluded that all the large isotope effect along with other salient features of phase transitions in HSQ as discussed above cannot be completely explained with a simple tunneling model [Eq. (1)] and considering elongation of the hydrogen bonds in DSQ as suggested by Samara and Semmingsen.[7] The actual mechanism of transition in HSQ is far more complicated.

Finally, we also conclude from the results of our theoretical investigations that there is a strong evidence of the crossover phenomenon in squaric acid which is also supported from the ^{13}C NMR studies made by Mehring and Mecker.[35] A crossover from first order to continuous phase transition induced by a symmetry-breaking field for a 2D model has also recently been proposed by Kerszberg and Mukamel.[21] Our theoretical results definitely provide strong support to the data of Kerszberg and Mukamel.[21] However, further experimental observation to confirm the crossover behavior in HSQ would definitely be interesting.

ACKNOWLEDGMENTS

One of the authors (B.K.C.) is grateful to Mr. K. K. Som, Dr. S. Banerjee, Dr. (Mrs.) K. Chaudhuri, and Dr. K. R. Choudhury for various help in the completion of this work.

[1]S. Cohen, J. Am. Chem. Soc. **81**, 3480 (1959).
[2]D. Semmingsen and J. Feder, Solid State Commun. **15**, 1369 (1974).
[3]J. Feder, in *Oxocarbons*, edited by Robert West (Academic, New York, 1980), p. 141.
[4]J. Feder, Ferroelectrics **12**, 71 (1976).
[5]J. Petersson and H. D. Maier, Ferroelectrics **24**, 157 (1980).
[6]See, for example, M. E. Lines and A. M. Glass, in *Principles and Applications of Ferroelectrics and Related Materials* (Clarendon, Oxford, 1977), p. 300.
[7]G. A. Samara and D. Semmingsen, J. Chem. Phys. **71**, 1401 (1979).
[8]D. Semmingsen, F. J. Hollanden, and T. F. Koetzle, J. Chem. Phys. **66**, 4405 (1977).
[9]N. Yasuda, K. Sumi, H. Shimizu, S. Fuzimoto, and Y. Inuishi, Jpn. J. Appl. Phys. **18**, 1485 (1979).
[10]E. Eatsushita, K. Yshimitsu, and T. Matsubara, Prog. Theor. Phys. **64**, 1177 (1980).
[11]V. I. Zinenko, Phys. Status Solidi B **78**, 721 (1976).
[12]V. E. Schneider and E. E. Tornau, Phys. Status Solidi B **107**, 491 (1981).
[13]S. Ganguli, D. Nath, and B. K. Chaudhuri, Phys. Rev. B **21**, 2937 (1980).
[14]B. K. Chaudhuri, S. Ganguli, T. Atake, and H. Chihara, J. Phys. Soc. Jpn. **49**, 608 (1980).
[15]B. K. Chaudhuri, S. Banerjee, and D. Nath, Phys. Rev. B **23**, 2308 (1981).
[16]S. Banderjee, D. Nath, and B. K. Chaudhuri, Phys. Rev. B **24**, 6469 (1982); **25**, 1883 (1982).
[17]E. J. Samuelsen and D. Semmingsen, Solid State Commun. **17**, 217 (1975).
[18]J. D. Becker, D. Suwelack, and M. Mehring, Solid State Commun. **25**, 1145 (1978).
[19]M. Mehring and D. Suwelack, Phys. Rev. Lett. **42**, 317

(1979).
[20]W. Kuhn, H. D. Maier, and J. Petersson, Solid State Commun. **32**, 249 (1979).
[21]M. Kerszberg and D. Mukamel, Phys. Rev. Lett. **43**, 293 (1979).
[22]S. Havlin, E. Litov, and H. Sompolinsky, Phy. Rev. B **13**, 4999 (1976).
[23]J. P. Harrison, J. P. Hessler, and D. R. Taylor, Phys. Rev. B **14**, 2979 (1976).
[24]G. A. Samara (unpublished); see also Ref. 7.
[25]Y. Wang and G. D. Stucky, J. Chem. Soc. Perkin Trans. II, 925 (1974).
[26]D. Semmingsen, Tetrahedron Lett. **807** (1973); Acta. Chem. Scand. **27**, 3961 (1973).
[27]M. F. Sykees and M. E. Fisher, Physica **28**, 919 (1962); **28**, 939 (1962).
[28]R. Blinc and S. Svetina, Phys. Rev. **147**, 423 (1966).
[29]S. Havlin, E. Litov, and H. Sompolinsky, Phys. Rev. B **14**, 1297 (1976); Y. Ishibashi, S. Ohya, and Y. Takagi, J. Phys. Soc. Jpn. **33**, 1545 (1972).
[30]N. Zubarev, Usp. Fiz. Nauk **70**, 585 (1960) [Sov. Phys.—Usp. **3**, 230 (1960)].
[31]V. L. Bonch Bruevich and S. V. Tyablikov, in *The Green's Function Method in Statistical Mechanics* (North-Holland, Amsterdam, 1962).
[32]K. K. Kobayashi, J. Phys. Soc. Jpn. **24**, 497 (1968).
[33]P. S. Peercy and G. A. Samara, Phys. Rev. B **8**, 2033 (1973).
[34]M. E. Fisher, Philos. Mag. **7**, 1731 (1962).
[35]M. Mehring and J. D. Becker, Phys. Rev. Lett. **47**, 366 (1981).
[36]F. Gronvold, J. Pure Appl. Chem. **47**, 252 (1976).
[37]D. Barth, J. Helwing, D. H. Maier, H. E. Musen, and J. Petersson, Z. Phys. B **34**, 393 (1979).
[38]W. Rehwald and A. Vonlanther, Phys. Status Solidi B **90**, 61 (1978).
[39]K. Ishida and A. M. Glazer, Ferroelectrics **6**, 293 (1974).
[40]R. Blinc, B. Zecks, and R. A. Talivrkheli, Phys. Rev. B **18**, 338 (1978).
[41]D. Suwelack and M. Mehring, Solid State Commun. **33**, 207 (1980).
[42]R. W. Whatmore, R. Clarke, and A. M. Clazer, J. Phys. C **11**, 3089 (1978).